# A Model for Nonclassical Nucleation of Solid-Solid Structural Phase Transformations

Y.A. CHU, B. MORAN, A.C.E. REID, and G.B. OLSON

A new model for homogeneous nucleation of structural phase transformations, which can span the range of nucleation from classical to nonclassical, is presented. This model is extended from the classical nucleation theory by introducing driving-force dependencies into the interfacial free energy, the misfit strain energy, and the nucleus chemical free-energy change in order to capture the nonclassical nucleation phenomena. The driving-force dependencies are determined by matching the asymptotic solutions of the new model for the nucleus size and the nucleation energy barrier to the corresponding asymptotic solutions of the Landau–Ginzburg model for nucleation of solid-state phase transformations in the vicinity of lattice instability. Thus, no additional material parameters other than those of the classical nucleation theory and the Landau–Ginzburg model are required, and nonclassical nucleation behavior can be easily predicted based on the well-developed analytical solutions of the classical nucleation model. A comparison of the new model to the Landau–Ginzburg model for homogeneous nucleation of a dilatational transformation is presented as a benchmark example. An application to homogeneous nucleation of a cubic-to-tetragonal transformation is presented to illustrate the capability of this model. The nonclassical homogeneous nucleation behavior of the experimentally studied fcc → bcc transformation in the Fe-Co system is examined by the new model, which predicts a 20 pct reduction in the critical driving force for homogeneous nucleation.

## I. INTRODUCTION

MARTENSITIC nucleation in solids has been extensively studied within the framework of the so-called classical nucleation theory (based on linear elasticity for evaluation of the self-energy associated with nucleation and on the assumption of a sharp interface with a constant interfacial free energy). The classical nucleation model[1–4] is known to accurately represent heterogeneous nucleation behavior in the vicinity of equilibrium.* Outside this regime, and especially as the condition for lattice instability** is approached, nonclassical nucleation is predicted.[5] Characteristic features of nonclassical nucleation in solid-state transformations which are not predicted by classical theory include the divergence of the size of the critical nucleus and the vanishing of the nucleation energy barrier as the condition for lattice instability is approached.

* At equilibrium, the potential wells associated with the parent and product phases have the same level of free-energy density.

** At lattice instability, the free-energy density barrier vanishes.

An alternative approach to modeling solid-state phase transitions is based on nonlinear, nonlocal elasticity and can be regarded as a Landau–Ginzburg-type approach wherein the Landau potential (nonconvex free-energy functional) is augmented by a gradient energy contribution resulting from a continuum description of material behavior at atomistic scales.[6] This approach is well suited to the study of critical phenomena associated with nonclassical nucleation and has been used in the context of one-dimensional nucleation problems by Olson and Cohen[7] and Haezebrouck.[8] Moran *et al.*[9] use a strain-based finite-element method together with a perturbed Lagrangian algorithm to study nucleation of a dilatational phase transformation for materials governed by a Landau–Ginzburg potential. Chu and Moran[10] use a displacement-based element-free Galerkin method,[11,12] in conjunction with a Landau–Ginzburg model in two dimensions, for nucleation of a deviatoric (square to rectangular) transformation.[13,14] The restriction to low-dimensional systems is a practical limitation of these spatially resolved methods, which do not favor closed-form analytical solutions. The applications mentioned previously are all numerical and, in two dimensions, tend to be computationally intensive.[10] This method has not been attempted for a true three-dimensional (3-D) system.

A new model, extended from the classical nucleation theory and spanning the range from classical to nonclassical nucleation, is introduced here. An attractive feature of this model is that closed-form analytical solutions can be obtained, making it simple to apply to realistic physical systems and to the study of the effects of model material parameters. The classical nucleation model can be modified to capture the nonclassical behavior by introducing appropriate driving-force dependencies into the interfacial free-energy density, the misfit strain energy per particle volume (*i.e.*, the so-called *self-energy* per particle volume), and the nucleus chemical free-energy change. These driving-force dependencies are determined by matching the asymptotic solutions of the new model for the nucleus size and the nucleation energy barrier to the corresponding asymptotic solutions of the Landau–Ginzburg model, shown in the Appendix, for nucleation of solid-state phase transformations near the highly nonclassical limit of lattice instability. Thus, no additional material parameters other than those of

Y.A. CHU, Researcher, is with the Chung-Shuan Institute of Science and Technology, Taiwan 32500, Republic of China. B. MORAN, Professor, Department of Civil Engineering, and G.B. OLSON, Professor, and A.C.E. REID, Research Associate, Department of Materials Science of Engineering, are with Northwestern University, Evanston, IL 60208.

Manuscript submitted July 28, 1998.

the classical nucleation model and the Landau–Ginzburg model are required, and nonclassical nucleation behavior can be easily predicted based on the well-developed analytical solutions of the classical nucleation model.

In the following sections, the classical nucleation model and the Landau–Ginzburg model are briefly reviewed, the new model is described, and the associated driving-force dependencies are derived. A comparison of the new model and the nonlinear, nonlocal Landau–Ginzburg model, for the particular case of homogeneous nucleation of a dilatational transformation, is presented to illustrate the capability of the model. An application to homogeneous nucleation of a cubic-to-tetragonal transformation is then presented, and the nonclassical nucleation behavior is discussed. The model is also applied to an experimentally accessible system, the nonclassical homogeneous nucleation of the fcc → bcc transformation (previously investigated experimentally by Lin *et al.*[15]) in the Fe-Co system. The asymptotic solutions of the Landau–Ginzburg model in the vicinity of lattice instability are derived in the Appendix.

## II. NUCLEATION MODELS

### A. *Classical Nucleation Model*

We begin with the standard classical analysis of homogeneous, coherent nucleation in solids.[1–4] The total free-energy change due to formation of a coherent nucleus (the product phase) in a homogeneous solid (the parent phase) is written as

$$\Delta G = (\Delta \hat{G}_s + \Delta G_v)\hat{V} + \hat{\Gamma}\hat{S} \qquad [1]$$

where $\Delta \hat{G}_s$ is the misfit strain energy per particle volume, $\Delta G_v$ is the chemical free-energy density change (*i.e.*, the difference in free-energy densities of the parent phase and a fully developed product phase, which is negative), $\hat{\Gamma}$ is the interfacial free-energy density, $\hat{V}$ is the volume of the nucleus, and $\hat{S}$ is the surface area of the nucleus. The absolute value of the chemical free-energy density change ($|\Delta G_v|$) is the so-called *driving force* for nucleation. The misfit strain energy is a consequence of the accommodation of the elastically deformed nucleus in the host lattice. That this term is proportional to the nucleus volume has been demonstrated in the inclusion work of Eshelby.[16] This term is also proportional to the square of the misfit strain and depends on the nucleus shape in a fairly complicated way.[16,17,18] For the simplest case of a spherical nucleus with a radius of $a$, Eq. [1] becomes

$$\Delta G = \frac{4}{3}\pi a^3(\Delta \hat{G}_s + \Delta G_v) + 4\pi a^2\hat{\Gamma} \qquad [2]$$

The critical nucleus is obtained at the radius $a^*$, for which Eq. [2] has zero derivative with respect to $a$, giving

$$a^* = \frac{2\hat{\Gamma}}{-(\Delta G_v + \Delta \hat{G}_s)} \qquad [3]$$

$$\Delta G^* = \frac{16\pi\hat{\Gamma}^3}{3(\Delta G_v + \Delta \hat{G}_s)^2} \qquad [4]$$

where $\Delta G^*$ is the nucleation energy barrier corresponding to the critical radius $a^*$.

In classical nucleation theory, the interfacial energy density and the misfit strain energy are constants independent of the driving force for the transformation. For $\Delta G_v = -\Delta \hat{G}_s$, the driving force at which coherent transformation becomes thermodynamically possible, the critical nucleus size and energy barrier predicted by the classical theory are infinite. As the driving force $|\Delta G_v|$ increases, the critical nucleus size and energy barrier decrease, but remain finite for a finite value of the chemical free-energy density change. Since instability of the parent lattice occurs at a finite driving force, this simple model necessarily loses validity in this nonclassical regime and fails to reproduce nonclassical effects such as the divergence in the nucleus size and a vanishing of the nucleation energy barrier in the vicinity of lattice instability.

### B. *Landau–Ginzburg Model*

An alternative approach to nucleation theory, well suited to nonclassical nucleation phenomena, is that of Cahn and Hilliard,[19] who used a Landau–Ginzburg-type model for nucleation in a two-component fluid. A general form of the nucleation energy barrier, based on the Landau–Ginzburg model for the particular case of solid-state phase transformations, is written as[6,7,13,14]

$$\Delta G = \int_\Omega (g(\eta_\gamma, \alpha) + \psi(\nabla\eta_\gamma))\, d\Omega \qquad [5]$$

where $\Omega$ represents an infinite domain. The quantity $g(\eta_\gamma, \alpha)$ is the Landau free-energy density, or thermodynamic potential, corresponding to the bulk terms ($\Delta \hat{G}_s + \Delta G_v$) of Eq. [1]. This quantity will have multiple local minima at different values of $\eta_\gamma$. The term $\psi(\nabla\eta_\gamma)$ is the strain-gradient energy corresponding to the interfacial energy in the classical nucleation model. The quantities of $\eta_\gamma$ are the strain-order paramters, indexed by the subscript $\gamma$; $\nabla$ is the spatial-gradient operator; and $\alpha \equiv \Delta G_v/\Delta G_{vi}$ is the normalized transformation driving force, which is 0 at equilibrium and 1 at lattice instability. The denominator $\Delta G_{vi} = g(\eta_\gamma, \alpha)|_{\eta_\gamma=1,\alpha=1} - g(\eta_\gamma, \alpha)|_{\eta_\gamma=0,\alpha=1}$ is the critical driving force for lattice instability (*i.e.*, the difference in bulk free-energy densities of the parent phase ($\eta_\gamma = 0$) and the fully developed product phase ($\eta_\gamma = 1$) at lattice instability ($\alpha = 1$)).

For a dilatational transformation with spherical symmetry, the 2-3-4 Landau–Ginzburg potential is written as[9]

$$\Delta G = 4\pi \int_0^\infty \left( g(\eta, \alpha) + \frac{2}{3}\mu\eta^2 + \frac{\kappa}{2}\left(\frac{d\eta}{dr}\right)^2 \right) r^2\, dr \qquad [6]$$

where $g(\eta, \alpha) = A\eta^2 - B\eta^3 + C\eta^4$ is the 2-3-4 Landau potential of dilatational deformation, the order parameter $\eta$ is the normalized dilatation strain, and $A$, $B$, $C$, $\mu$, and $\kappa$ are material constants. The dependence of the 2-3-4 potential function on the normalized driving force is depicted in Figure 1. The well center at $\eta = 0$ represents the parent phase, and the well center at $\eta = 1$ represents a fully developed product phase. The driving force in energy units, *i.e.*, the difference between the bulk free-energy densities of the parent phase and those of a fully developed product phase, is given as a function of the *normalized* driving force by $g(1, \alpha)$. Traveling along the energy surface $g(\eta)$ in the direction of the order parameter $\eta$, the height of the energy barrier encountered is given by $\phi$. This quantity decreases as the normalized driving force increases and is denoted by $\phi_0$ at equilibrium

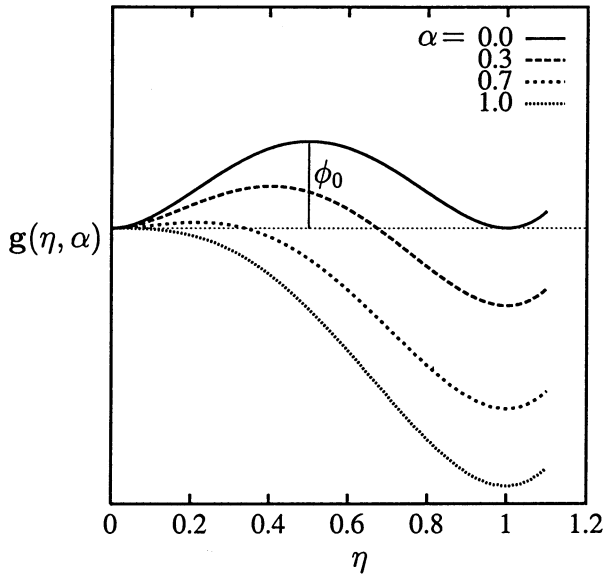


Fig. 1—Landau 2-3-4 potential $g(\eta, \alpha)$ for different values of the normalized driving force $\alpha$.

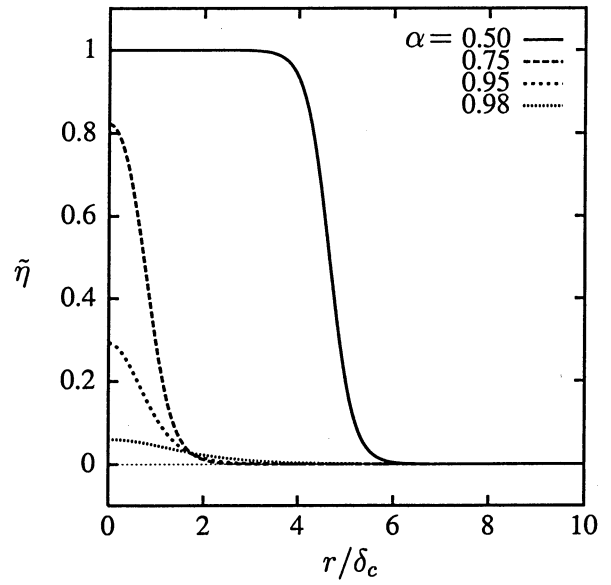


Fig. 2—Normalized strain profiles for critical nuclei, $\tilde{\eta}(r)$, for different values of the normalized driving force $\alpha$.[9]

($\alpha = 0$). The critical nucleus is obtained through stationarity of Eq. [6] with respect to the order parameter $\eta$, which, in this case, is a function of the spatial coordinates of the system.

Moran *et al.*[9] use a strain-based finite-element method together with a perturbation scheme to solve the weak form of Eq. [6]. The numerical solutions are briefly reviewed as follows: in Figure 2, the normalized strain profiles* for critical nuclei ($\tilde{\eta}(r)$) are plotted, as a function of the normalized radius $r/\delta_c$ for different values of the normalized driving force, with the Poisson's ratio $\nu = 0.45$. Because the Landau–Ginzburg theory is a continuum theory, there is no characteristic length scale in the model system except that induced by the presence of gradient terms in Eq. [6]. In order to provide a physically meaningful measure of length, we introduce the quantity

$$\delta_c \equiv \left( \sqrt{\frac{\kappa}{2C}} \frac{8C}{B} \right) \Bigg|_{\alpha = \alpha_{c0}} \qquad [7]$$

which is the interface thickness at coherent equilibrium.*

* The strain-order parameter is rescaled for the combined Landau potential ($g(\eta, \alpha) + 2/3\ \mu\eta^2$) to have a minimum at $\overline{\eta} = 1$.[9]

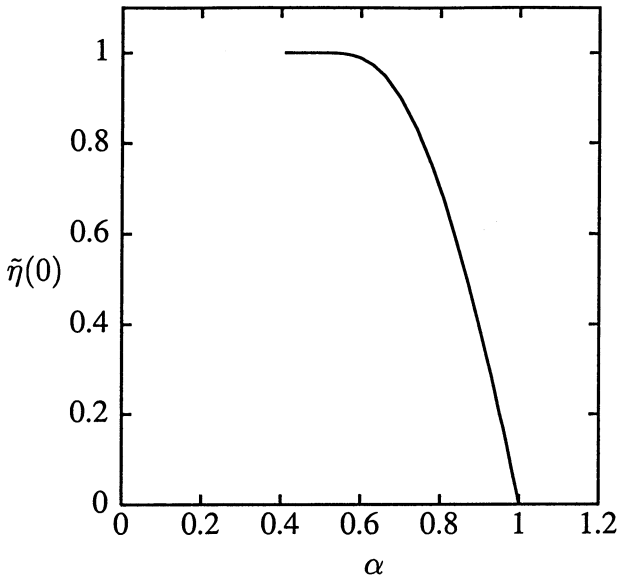


Fig. 3—Normalized center strain $\tilde{\eta}(0)$ for the critical nucleus as a function of the normalized driving force $\alpha$.[9]

* Due to the shear resistance, the dilatational transformation under conditions of inhomogeneous deformation requires a higher driving force than that of the transformation under conditions of homogeneous deformation and first becomes thermodynamically possible at coherent equilibrium with the normalized driving force ($\alpha = \alpha_{c0}$), which depends on the value of the Poisson's ratio ($\nu$).[9]

For the case of $\nu = 0.45$, the value of the normalized driving force at coherent equilibrium is $\alpha_{c0} = 0.4$. It can be seen from Figure 2 that, as $\alpha \rightarrow \alpha_{c0} = 0.4$ (for example, $\alpha = 0.5$), the normalized strain is uniform within the nucleus, with a sharp decrease in strain over a narrow range, indicating a sharp interface. In contrast, as $\alpha \rightarrow 1$ (for example, $\alpha = 0.98$), the normalized strain profile is nonuniform within the nucleus and the strain transition occurs over a broader range, indicating a more diffuse, nonclassical interface. The intermediate cases, $\alpha = 0.75$ and 0.95, have nonuniform strain profiles and relatively sharp interface thicknesses.

Another indicator of classical *vs* nonclassical behavior, valuable in the construction of the extended theory, is the normalized center strain of a critical nucleus. In Figure 3, this quantity is plotted as a function of normalized driving force. The normalized center strain decreases as the driving force increases. As $\alpha \rightarrow \alpha_{c0} = 0.4$, the spherical nucleus structure, which has $\tilde{\eta}(0) = 1$, has the fully developed product phase in its interior, characteristic of classical behavior. As $\alpha \rightarrow 1$, the nucleus structure, which has $\tilde{\eta}(0) \rightarrow 0$, becomes indistinguishable from the parent structure and the behavior is strongly nonclassical.

The radius ($R$) of the critical nucleus can be defined by $|\eta'|_{r=R} = |\eta'|_{\max}$ (where a prime symbol denotes differentiation with respect to $r$), which means that the maximum strain

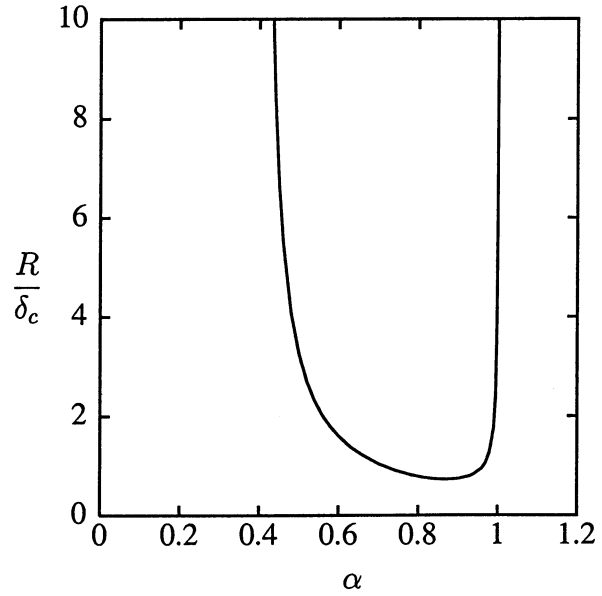


Fig. 4—Radius $R$ of the critical nucleus, normalized with respect to $\delta_c$, as a function of the normalized driving force $\alpha$.[9]

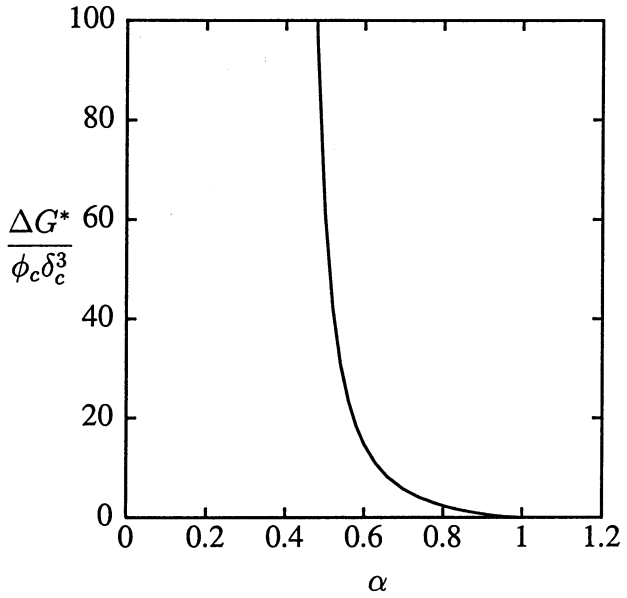


Fig. 5—Nucleation energy barrier $\Delta G^*$ of the critical nucleus, normalized with respect to $\phi_c\delta_c^3$, as a function of the normalized driving force $\alpha$.[9]

gradient occurs at $r = R$. Since strain gradients are costly in energy, the maximal strain gradient will occur where the system is locally unable to access either the parent or product-state wells. This transitional region is, thus, a natural choice for the boundary of the nucleus. In Figure 4, the radius of the critical nucleus, normalized with respect to the interface thickness defined in Eq. [7], is plotted as a function of the normalized driving force. The radius of the critical nucleus, which is infinite in the classical limit of coherent equilibrium ($\alpha = \alpha_{c0}$), is seen to decrease initially to a minimum, then to increase and become infinite again at lattice instability ($\alpha = 1$). The phenomenon of $R \rightarrow \infty$ as $\alpha \rightarrow 1$ is an important feature of the nonclassical nucleation, which is not present in the classical model.

In Figure 5, the nucleation energy barrier of the critical nucleus, normalized with respect to $\phi_c\delta_c^3$, is plotted as a function of the normalized driving force, where $\phi_c$ is the energy-density barrier at coherent equilibrium. The nucleation energy barrier is infinite at coherent equilibrium, but decreases rapidly as the driving force increases and tends to zero as lattice instability ($\alpha = 1$) is approached. The vanishing of the nucleation energy barrier at lattice instability is another important feature of the nonclassical nucleation which is not observed in the classical model.

It is shown in the Appendix that, based on a 2-3-4 Landau–Ginzburg potential,[7]* the asymptotic solutions for the radii of the critical nucleus ($R_j^*$) and the nucleation energy barrier in the vicinity of lattice instability ($\alpha = 1$) are

$$R^*_{j(\alpha\rightarrow 1)} \sim (1 - \alpha)^{-1/2} \quad [8]$$

$$\Delta G^{2-3-4}_{(\alpha\rightarrow 1)} \sim (1 - \alpha)^{3/2} \quad [9]$$

The existing nonclassical theory does not lend itself to closed-form analytical solutions. In addition, numerical solutions in two dimensions are computationally intensive[10] and have not been attempted in three dimensions.

* It is also shown in the Appendix that the asymptotic solutions of a 2-4-6 Landau–Ginzburg potential[13,14] have a different asymptotic behavior in the nucleation energy barrier as $\Delta G^{2-4-6}_{(\alpha\rightarrow 1)} \sim (1 - \alpha)^{1/2}$, but have the same asymptotic behavior in the radii of the critical nucleus as that shown in Eq. [8].

### C. *Nonclassical Nucleation Model*

Comparing the solutions of the classical nucleation model for a dilatational transformation (Eqs. [3] and [4]) to the corresponding asymptotic solutions of the Landau–Ginzburg model (Eqs. [8] and [9]), it is found that, in order to capture the nonclassical nucleation behavior shown in Eqs. [8] and [9], appropriate driving-force dependencies in the interfacial energy density, the misfit strain energy per particle volume, and the chemical free-energy density change are required in Eqs. [3] and [4]. Reviewing the solutions of the Landau–Ginzburg models[7–10] and also referring to Figures 1 through 5, the strain-gradient energy density ($\psi$) corresponding to the interfacial energy density, the amplitude of strains within the nucleus representing the nucleus structure, and the free-energy density barrier relating to the misfit strain energy per particle volume all decrease as the driving force increases. Based on the previous observations, we propose the following driving-force dependencies for the interfacial energy density and the misfit strain energy per particle volume:

$$\hat{\Gamma} = \Gamma(1 - \alpha)^m \quad [10]$$

$$\Delta\hat{G}_s = \Delta G_s(1 - \alpha)^n \quad [11]$$

where $\Gamma$ and $\Delta G_s$ are the interfacial energy density and the misfit strain energy per particle volume at equilibrium ($\alpha = 0$), respectively, and $m$ and $n$ are parameters to be determined.

Referring to the Landau potential depicted in Figure 1 and considering that the amplitude of strains within the nucleus ($\bar{\eta}(0)$) decreases as the driving force increases (presented in Figure 3), the *nucleus chemical free-energy density change* ($\Delta\hat{G}_v$), *i.e.*, the difference in the free-energy densities of the parent phase and a of nonfully developed product phase associated with nonclassical nucleation, corresponding to $g(\eta, \alpha)|_{\eta=\eta(0)}$, where $\eta(0)$ represents the center strain

of the nucleus, first increases and then decreases as $\alpha$ increases and $\eta(0)$ decreases. Therefore, the the driving-force dependency for the nucleus chemical free-energy density change is proposed to be

$$\Delta\hat{G}_v = \Delta G_v\,(1 - \alpha)^n = \Delta G_{vi}\alpha(1 - \alpha)^n \qquad [12]$$

where $\Delta G_v = \Delta G_{vi}\alpha$ is the chemical free-energy density change (*i.e.*, the difference in free-energy densities of the parent phase and of a fully developed product phase) adopted in the classical nucleation model.* The nucleus chemical free-energy density change is linearly proportional to the normalized driving force in the vicinity of equilibrium and has the same driving-force dependence as the misfit strain energy per particle volume in the vicinity of lattice instability.** Substituting Eqs. [10] through [12] into Eq. [1], replacing $\Delta G_v$ by $\Delta\hat{G}_v$, yields

$$\Delta G = (1 - \alpha)^n(\Delta G_s + \Delta G_{vi}\alpha)\hat{V} + (1 - \alpha)^m\Gamma\hat{S} \qquad [13]$$

Considering the asymptotic solution of the radii of the critical nucleus shown in Eq. [8], the asymptotic behavior in the volume and the surface area of the critical nucleus near lattice instability is

$$\hat{V}_{\alpha\to 1} \sim (1 - \alpha)^{-s/2} \qquad [14]$$

$$\hat{S}_{\alpha\to 1} \sim (1 - \alpha)^{-(s-1)/2} \qquad [15]$$

where $s$ represents the spatial dimensions associated with the considered transformations (*i.e.*, $s = 1$, 2, or 3 for one, two, or three dimensions, respectively). Therefore, the nucleation energy barrier near lattice instability in Eq. [13] is rewritten as

$$\begin{aligned}\Delta G_{\alpha\to 1} &= (1 - \alpha)^{(n-s/2)}(\Delta G_s + \Delta G_{vi}\alpha)V \\ &\quad + (1 - \alpha)^{(m+1/2-s/2)}\Gamma S \qquad [16]\\ &\sim (1 - \alpha)^{(n-s/2)} \quad \text{or} \quad (1 - \alpha)^{(m+1/2-s/2)} \qquad [17]\end{aligned}$$

where $V = \hat{V}_{\alpha\to 1}(1 - \alpha)^{s/2}$ and $S = \hat{S}_{\alpha\to 1}(1 - \alpha)^{(s-1)/2}$. In the Landau–Ginzburg case (Eq. [A.4]), the normalized Landau free energy and the strain-gradient energy have the same asymptotic behavior near the lattice instability. Assuming that the corresponding quantities, namely, the misfit strain energy and interfacial energy, also have the same asymptotic behavior, we find that

$$n = m + \frac{1}{2} \qquad [18]$$

Comparing Eqs. [17] and [18] to the asymptotic solutions of the Landau–Ginzburg model for the rate of convergence in the nucleation energy barrier shown in the Appendix, the values of the parameters $m$ and $n$ are determined. For example, comparing Eqs. [17] and [18] to [A.5] (or to Eq. [9] for $s = 3$) yields the values of $m = 2.5$ and $n = 3$. This enables the new model to have the same asymptotic solutions as those of a 2-3-4 Landau–Ginzburg model for transformations from one to three dimensions.

## III. BENCHMARK EXAMPLE: NUCLEATION OF A DILATATIONAL TRANSFORMATION

Hong[20] used a nonlocal model with a so-called *two-parabola* strain-energy density, that is, an energy surface consisting of either a parabola centered on the parent phase or one centered on the product phase, depending on which is lower in energy at the given strain. This energy was augmented by a strain-gradient energy density and was used to model homogeneous nucleation of a solid-solid dilatational transformation. Although the two-parabola model, which can be classified as a linear nonlocal model, lends itself to an analytical solution, it does not reproduce all of the critical phenomena associated with nonclassical nucleation, especially the divergence of nucleus size in the vicinity of lattice instability. Moran *et al.*[9] used a 2-3-4–type Landau–Ginzburg potential to study the same problem and solved the nonlinear nonlocal model, as described in Section II–B.

In this section, a comparison of the new model to a 2-3-4 Landau–Ginzburg model[9] for homogeneous nucleation of a dilatational transformation is presented. Considering nucleation of a spherical nucleus resulting from misfit dilatational strain, ($\hat{\epsilon}^*_{kk}$), the associated misfit strain energy per particle volume is

$$\Delta\hat{G}_s = 2\hat{K}\hat{\mu}(\hat{\epsilon}^*_{kk})^2/(3\hat{K} + 4\hat{\mu}) \qquad [19]$$

where $\hat{K}$ and $\hat{\mu}$ are the elastic bulk modulus and the shear modulus, respectively.[16,18] Considering the assumption of linear driving-force dependencies of the elastic moduli in the 2-3-4 model, implying $\hat{K} \sim (1 - \alpha)$ and $\hat{\mu} \sim (1 - \alpha)$ in Eq. [19] or $\hat{E}_{ijkl} \sim (1 - \alpha)$ from the Eshelby computation, and then comparing the result to Eq. [11] for the driving-force dependency in the misfit strain energy per particle volume (*i.e.*, $\Delta\hat{G}_s \to (1 - \alpha)^n$), yields

$$\hat{\epsilon}^*_{ij} \sim \epsilon^*_{ij}(1 - \alpha)^{(n-1)/2} \qquad [20]$$

where $\hat{\epsilon}^*_{ij}$ are the misfit strains at equilibrium ($\alpha = 0$). Based on the Eshelby solutions of strains within a particle and on Eq. [20], the normalized strains of the critical nucleus ($\tilde{\epsilon}_{ij}$) are defined as

$$\begin{aligned}\tilde{\epsilon}_{ij} &= \frac{\hat{\epsilon}_{ij}}{\hat{\epsilon}_{ij}\big|_{\alpha=\alpha_{c0}}} \text{ (no summation in } i \text{ and } j\text{)}\\ &= \frac{(1 - \alpha)^{(n-1)/2}}{(1 - \alpha_{c0})^{(n-1)/2}} \qquad [21]\end{aligned}$$

which are 1 at coherent equilibrium ($\alpha = \alpha_{c0}$) and 0 at lattice instability ($\alpha = 1$).

The radius of the critical nucleus and the nucleation energy barrier for a dilatational transformation are represented by Eqs. [3] and [4] (replacing $\Delta G_v$ by $\Delta\hat{G}_v$). Substituting Eqs. [10] through [12] into Eqs. [3] and [4] yields

$$a^* = \frac{2\Gamma}{-\Delta G_{vi}(\alpha - \alpha_{c0})(1 - \alpha)^{(n-m)}} \qquad [22]$$

$$\Delta G^* = \frac{16\pi\Gamma^3(1 - \alpha)^{(3m-2n)}}{3\Delta G_{vi}^2(\alpha - \alpha_{c0})^{2n}} \qquad [23]$$

where $\alpha_{c0} = -\Delta G_s/\Delta G_{vi}$ is the normalized driving force at coherent equilibrium, at which the dilatational transformation can first occur under conditions of inhomogeneous deformation.[9] In other words, the driving force for nucleation of a dilatational transformation is reduced by the misfit

* Note that $\Delta G_{vi}$ corresponds to the 2-3-4 Landau potential evaluated at the order parameter $\eta = 1$ and the normalized driving force $\alpha = 1$.

** Because the terms ($\Delta\hat{G}_s + \Delta\hat{G}_v$) correspond to the Landau free-energy density in Eq. [5], we assume that $\Delta\hat{G}_v$ and $\Delta\hat{G}_s$ have the same driving-force dependence in the vicinity of lattice instability.

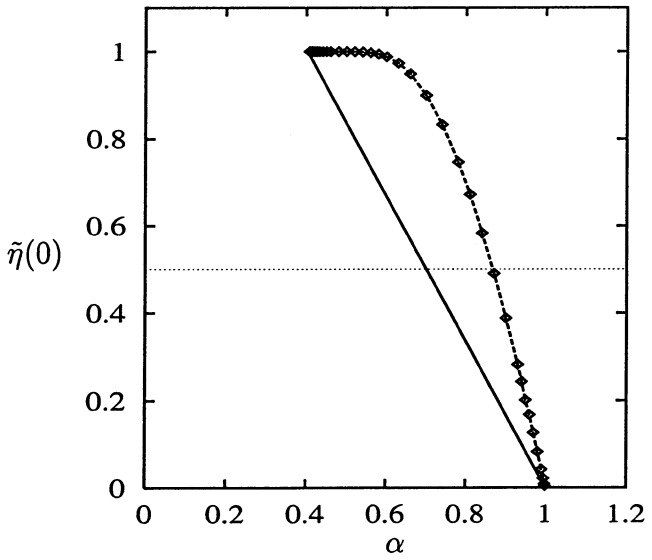


Fig. 6—Normalized center strain for the critical nucleus plotted as functions of the normalized driving force, $\alpha$, for a dilatational transformation. The solid line for the new model and the dashed line with symbols for the nonlinear nonlocal model.[9]

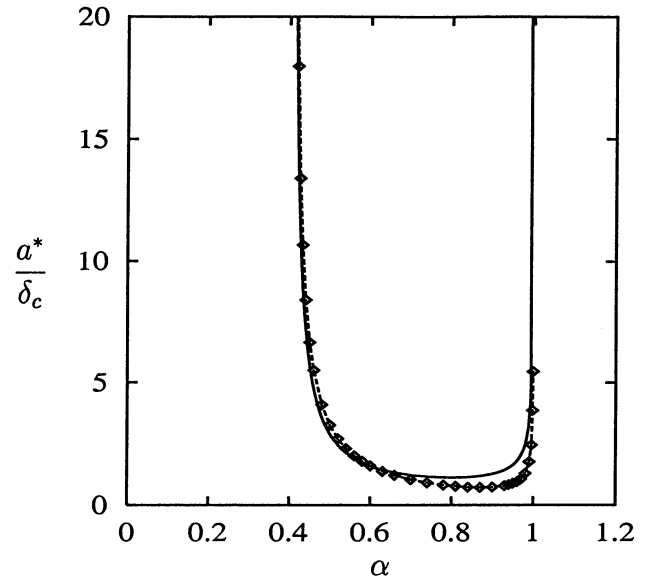


Fig. 7—Normalized radius of the critical nucleus plotted as functions of the normalized driving force; $\alpha$, for a dilatational transformation. The solid line for the new model and the dashed line with symbols for the nonlinear nonlocal model.[9]

strain energy associated with the accommodation by the parent phase.

Comparisons of Eqs. [21] through [23] to the numerical solutions in Moran *et al.*[9] for the normalized center strain ($\tilde{\eta}(0) = \tilde{\epsilon}_{kk}$), the radius of the critical nucleus and the nucleation energy barrier, depicted in Figures 3 through 5 for the case of a Poisson's ratio of $\nu = 0.45$, are shown in Figures 6 through 8, respectively. The radius of the critical nucleus and the nucleation energy barrier are normalized with respect to $\delta_c$ and $\delta_c^3\phi_c$, respectively, where $\delta_c$ and $\phi_c$ are the interface thickness and the free-energy density barrier at equilibrium, respectively.[9] The values of $m = 2.5$, $n = 3$, $\alpha_{c0} = 0.4$, $\Gamma = (8/5\pi)\delta_c\phi_c$, and $\Delta G_{vi} = -(16/\pi)\phi_c$ are used for the purpose of comparison.*

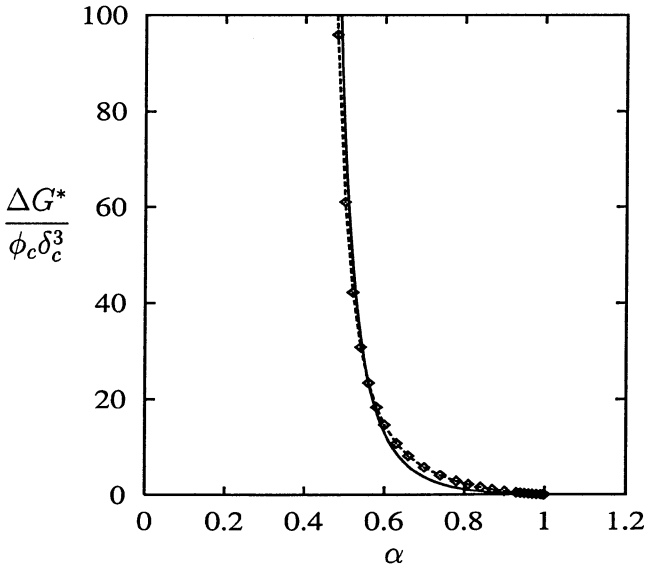


Fig. 8—Normalized nucleation energy barrier plotted as a function of the normalized driving force, $\alpha$, for a dilatational transformation. The solid line for the new model and the dashed line with symbols for the nonlinear nonlocal model.[9]

* The value of $\Delta G_{vi} = \beta\phi_0$ for $\beta = -3$ is adopted.

In Figure 6, the normalized center strain predicted by the new model (*i.e.*, $\tilde{\eta}(0) = \tilde{\epsilon}_{kk}$ in Eq. [21]) is simply represented by a straight line, in this case, varying from 1 at $\alpha = \alpha_{c0}$ to 0 at $\alpha = 1$, which is significantly different from that predicted by the 2-3-4 Landau–Ginzburg model, except at the end points. Following the classification of nucleation based on the normalized center strain by Olson and Roitburd,[5] a dashed line with $\tilde{\eta}(0) = 0.5$ is plotted for reference and classification in Figure 6. The transformations are regarded as a modification of classical nucleation for $\tilde{\eta}(0) > 0.5$ and as nonclassical for $\tilde{\eta}(0) < 0.5$. The value of the normalized driving force corresponding to $\tilde{\eta}(0) = 0.5$ can be easily predicted by the new model, based on Eq. [21], to be $\alpha = (\alpha_{c0} + 1)/2 = 0.7$, which is about 0.85 for the 2-3-4 Landau–Ginzburg model.

In Figure 7, the radius of the critical nucleus, normalized with respect to $\delta_c$, is plotted as a function of the normalized driving force. The radius of the critical nucleus, which is infinite at coherent equilibrium ($\alpha = \alpha_{c0}$), is seen to decrease initially to a minimum, then to increase and become infinite again at lattice instability ($\alpha = 1$). The phenomenon of $a^* \to \infty$ as $\alpha \to 1$ is an expected feature of the nonclassical nucleation which is not observed in the classical model. Both the new model and the nonlinear nonlocal model predict the same asymptotic solutions for $a^* \sim (\alpha - \alpha_{c0})^{-1}$ in the vicinity of coherent equilibrium and for $a^* \sim (1 - \alpha)^{-1/2}$ in the vicinity of lattice instability and match well within these two limits.

In Figure 8, the nucleation energy barrier of the critical nucleus, normalized with respect to $\delta_c^3\phi_c$, is plotted as a function of the normalized driving force. The nucleation energy barrier is infinite at coherent equilibrium ($\alpha = \alpha_{c0}$), but decreases rapidly as the value of $\alpha$ increases and tends to zero as lattice instability ($\alpha = 1$) is approached. The

vanishing of the nucleation energy barrier at lattice instability is another feature of nonclassical nucleation which is not observed in the classical model. Both the new model and the nonlinear nonlocal model predict the same asymptotic solutions for $\Delta G^* \sim (\alpha - \alpha_{c0})^{-2}$ in the vicinity of coherent equilibrium and for $\Delta G^* \sim (1 - \alpha)^{3/2}$ in the vicinity of lattice instability and again match well within these two limits.

## IV. APPLICATIONS

### A. *Cubic-to-Tetragonal Transformation*

The cubic-to-tetragonal phase transformation is of special interest in martensitic nucleation due to its importance in steels. A Landau–Ginzburg free-energy functional for modeling homogeneous nucleation of a cubic-to-tetragonal phase transformation can be found in Barsch and Krumhansl[13] and Hong and Olson.[21] Chu and Moran[10] presented a methodology for numerical simulation of nucleation of an analogous two-dimensional (2-D) (square to rectangular) deviatoric phase transformation. The numerical framework, based on the element-free Galerkin method,[11,10] is directly applicable to the 3-D cubic-to-tetragonal phase transformation but is computationally prohibitive. Consequently, we extended the new analytic model to the 3-D cubic-to-tetragonal phase.

Consider a cubic-to-tetragonal transformation resulting from misfit strains,

$$(\hat{\epsilon}^*_{ij}) = \hat{\epsilon}^*_{11}\begin{pmatrix} 1 & 0 & 0 \\ 0 & 1 & 0 \\ 0 & 0 & 1+\zeta \end{pmatrix} \qquad [24]$$

where $\zeta$ is a measure of the tetragonality of the transformation. The misfit strains in Eq. [24] are based on a coordinate system whose axes lie along the fourfold rotational axes of the cubic lattice. The preferred habit plane of a coherent particle is determined by minimization of the misfit strain energy per particle volume (*i.e.*, the self-energy density) with respect to the orientation of the habit plane (Khachaturyan, 1983[25]). Let $\mathbf{n} = n_i\mathbf{e}_i$ be the outward unit normal to the habit plane, where $\mathbf{e}_i$ represents the base vectors aligned with the crystal axes and $\mathbf{e}_3$ is in the direction of the tetragonal axis. For isotropic materials, the angle between the outward unit normal ($\mathbf{n}$) of the habit plane and the tetragonal axis ($x_3$) is $\theta = \cos^{-1}n_3$, where[22]

$$n_3^2 = \begin{cases} 1 + (3\lambda + 2\mu)/((2\lambda + 2\mu)\zeta) & -\infty \le \zeta \le -(3\lambda + 2\mu)/(2\lambda + 2\mu) \\ 0 & -(3\lambda + 2\mu)/(2\lambda + 2\mu) < \zeta < 0 \\ 1 & 0 < \zeta < \infty \end{cases} \qquad [25]$$

and where $\lambda$ and $\mu$ are the Lamé constants. The orientation of the habit plane is otherwise arbitrary, with $n_1$ and $n_2$ required only to satisfy the constraint

$$n_1^2 + n_2^2 = 1 - n_3^2 = \sin^2\theta \qquad [26]$$

Therefore, for isotropic materials, the orientation of the habit plane depends on the tetragonality ($\zeta$) and the material moduli $\lambda$ and $\mu$.

Considering nucleation of a thin oblate-spheroidal coherent nucleus, with radii of $a_1 = a_2 = a \gg a_3 = c$ aligned with a coordinate system ($\tilde{x}_1$, $\tilde{x}_2$, $\tilde{x}_3$) and with the $\tilde{x}_3$ axis in the direction of the outward unit normal to the habit plane, the misfit strain energy per particle volume resulting from misfit strains ($\hat{\epsilon}^*_{ij}$) is represented as[3,16]

$$\Delta\hat{G}_s = \Delta\hat{G}_{s1} + \Delta\hat{G}_{s2}\frac{c}{a} \qquad [27]$$

where

$$\Delta\hat{G}_{s1} = \mu\left(\frac{\nu}{1-\nu}(\hat{\epsilon}^*_{\tilde{1}\tilde{1}} + \hat{\epsilon}^*_{\tilde{2}\tilde{2}})^2 + (\hat{\epsilon}^*_{\tilde{1}\tilde{1}})^2 + (\hat{\epsilon}^*_{\tilde{2}\tilde{2}})^2 + 2(\hat{\epsilon}^*_{\tilde{1}\tilde{2}})^2\right) \qquad [28]$$

$$\begin{aligned}\Delta\hat{G}_{s2} = \frac{\pi\mu}{32(1-\nu)}\,&(8\nu(\hat{\epsilon}^*_{\tilde{1}\tilde{1}} + \hat{\epsilon}^*_{\tilde{2}\tilde{2}} + \hat{\epsilon}^*_{\tilde{3}\tilde{3}})(2\hat{\epsilon}^*_{\tilde{3}\tilde{3}} - \hat{\epsilon}^*_{\tilde{1}\tilde{1}} - \hat{\epsilon}^*_{\tilde{2}\tilde{2}}) \\ &- (13 - 8\nu)((\hat{\epsilon}^*_{\tilde{1}\tilde{1}})^2 + (\hat{\epsilon}^*_{\tilde{2}\tilde{2}})^2) + 2(1 - 8\nu)\hat{\epsilon}^*_{\tilde{1}\tilde{1}}\hat{\epsilon}^*_{\tilde{2}\tilde{2}} \\ &+ 8(1+\nu)(\hat{\epsilon}^*_{\tilde{1}\tilde{1}} + \hat{\epsilon}^*_{\tilde{2}\tilde{2}})\hat{\epsilon}^*_{\tilde{3}\tilde{3}} + 8(1 - 2\nu)(\hat{\epsilon}^*_{\tilde{3}\tilde{3}})^2 \\ &+ 16(2-\nu)((\hat{\epsilon}^*_{\tilde{2}\tilde{3}})^2 + (\hat{\epsilon}^*_{\tilde{3}\tilde{1}})^2) - 4(7 - 8\nu)(\hat{\epsilon}^*_{\tilde{1}\tilde{2}})^2)\end{aligned} \qquad [29]$$

For a cubic-to-tetragonal transformation resulting from the misfit strains in Eq. [24], the associated misfit strain energy (Eq. [27]) has a minimum if the misfit strains in Eqs. [28] and [29] satisfy

$$(\hat{\epsilon}^*_{\tilde{i}\tilde{j}}) = (R_{k\tilde{i}})^T\begin{pmatrix} \hat{\epsilon}^*_{11} & 0 & 0 \\ 0 & \hat{\epsilon}^*_{11} & 0 \\ 0 & 0 & \hat{\epsilon}^*_{11}(1+\zeta) \end{pmatrix}(R_{l\tilde{j}}) \qquad [30]$$

where $R_{i\tilde{j}}$ represents the coordinate transformation (rotation) tensors, defined as

$$\begin{aligned}(R_{i\tilde{j}})^T &= \begin{pmatrix} \tilde{\mathbf{e}}_1\cdot\mathbf{e}_1 & \tilde{\mathbf{e}}_1\cdot\mathbf{e}_2 & \tilde{\mathbf{e}}_1\cdot\mathbf{e}_3 \\ \tilde{\mathbf{e}}_2\cdot\mathbf{e}_1 & \tilde{\mathbf{e}}_2\cdot\mathbf{e}_2 & \tilde{\mathbf{e}}_2\cdot\mathbf{e}_3 \\ \tilde{\mathbf{e}}_3\cdot\mathbf{e}_1 & \tilde{\mathbf{e}}_3\cdot\mathbf{e}_2 & \tilde{\mathbf{e}}_3\cdot\mathbf{e}_3 \end{pmatrix} \\ &= \begin{pmatrix} \tilde{\mathbf{e}}_1\cdot\mathbf{e}_1 & \tilde{\mathbf{e}}_1\cdot\mathbf{e}_2 & \tilde{\mathbf{e}}_1\cdot\mathbf{e}_3 \\ \tilde{\mathbf{e}}_2\cdot\mathbf{e}_1 & \tilde{\mathbf{e}}_2\cdot\mathbf{e}_2 & \tilde{\mathbf{e}}_2\cdot\mathbf{e}_3 \\ n_1 & n_2 & n_3 \end{pmatrix}\end{aligned} \qquad [31]$$

and where $\tilde{\mathbf{e}}_3 = \mathbf{n}$ and $\tilde{\mathbf{e}}_1$ and $\tilde{\mathbf{e}}_2$ are two mutually orthogonal (but otherwise arbitrary) base vectors lying in the habit plane. Therefore, the minimum misfit strain energy per particle volume for a cubic-to-tetragonal transformation is evaluated by Eqs. [24] through [31].

For the thin oblate-spheroidal nucleus, the nucleation energy barrier of a cubic-to-tetragonal transformation in a linear elastic, isotropic material is

$$\Delta G = 2\pi a^2\hat{\Gamma} + \frac{4}{3}\pi a^2 c\left(\Delta\hat{G}_{s1} + \Delta\hat{G}_{s2}\frac{c}{a} + \Delta\hat{G}_v\right) \qquad [32]$$

Note that the term $\Delta\hat{G}_{s1}$ in Eq. [32] implies that part of the misfit strain energy per particle volume cannot be accommodated by varying the shape of the nucleus of the tetragonal phase. This is a significant difference between a simple shear transformation and a cubic-to-tetragonal transformation,[23] which illustrates the fundamentally 3-D character of the latter. The critical nucleus is then obtained through stationarity of Eq. [32] with respect to the radii $a$ and $c$, considering the driving-force dependencies of the interfacial free-energy density, the misfit strain energy per particle volume, and the nucleus chemical free-energy density change as shown in Eqs. [10] through [12], which yields

$$a^* = \frac{4\Gamma\Delta G_{s2}}{\Delta G_{vi}^2} \frac{1}{(\alpha - \alpha_{c0})^2(1 - \alpha)^{(n-m)}} \quad [33]$$

$$c^* = \frac{2\Gamma}{-\Delta G_{vi}} \frac{1}{(\alpha - \alpha_{c0})(1 - \alpha)^{(n-m)}} \quad [34]$$

$$\Delta G^* = \frac{32\pi\Gamma^3\Delta G_{s2}^2}{3\Delta G_{vi}^4} \frac{(1 - \alpha)^{(3m-2n)}}{(\alpha - \alpha_{c0})^4} \quad [35]$$

where $\Delta G_{s1} = \Delta\hat{G}_{s1}/(1 - \alpha)^n$, $\Delta G_{s2} = \Delta\hat{G}_{s2}/(1 - \alpha)^n$, and $\alpha_{c0} = -\Delta G_{s1}/\Delta G_{vi}$. The normalized center strains of the critical nucleus, for the case of linear driving-force dependencies in the elastic moduli, are represented by Eq. [21] as

$$\tilde{\epsilon}_{ij}(0) = \frac{(1 - \alpha)^{(n-1)/2}}{(1 - \alpha_{c0})^{(n-1)/2}} \quad [36]$$

The normalized center strains of the critical nucleus are linearly proportional to $(1 - \alpha)$ for $n = 3$.

In the vicinity of lattice instability, both radii of the critical nucleus ($a^*$ and $c^*$) have the same asymptotic behavior, *i.e.*, $a^* \sim (1 - \alpha)^{-1/2}$ and $c^* \sim (1 - \alpha)^{-1/2}$ for $m = 2.5$ and $n = 3$, which is consistent with the corresponding asymptotic solutions of the associated Landau–Ginzburg model shown in the Appendix. Close to coherent equilibrium ($\alpha \to \alpha_{c0}$), the asymptotic behavior is $a^* \sim (\alpha - \alpha_{c0})^{-2}$ and $c^* \sim (\alpha - \alpha_{c0})^{-1}$, which is consistent with the classical theory for martensitic nucleation.

The shape of the critical nucleus is represented by

$$\chi^* \equiv c^*/a^* = (-\Delta G_{vi}/2\Delta G_{s2})\,(\alpha - \alpha_{c0}) \quad [37]$$

The value of $\chi^*$ is linearly proportional to the normalized driving force, which is 0 at coherent equilibrium and $(-\Delta G_{vi}/2\Delta G_{s2})\,(1 - \alpha_{c0})$ at lattice instability. Thus, a very thin oblate-spheroidal nucleus is predicted in the vicinity of coherent equilibrium as in the classical theory, and a thicker oblate-spheroidal nucleus is expected in the regime of nonclassical nucleation.

The asymptotic behavior of the nucleation energy barrier in the vicinity of lattice instability ($\alpha \to 1$) is $\Delta G^* \sim (1 - \alpha)^{3/2}$, which is also consistent with the corresponding asymptotic solutions of the associated Landau–Ginzburg model shown in the Appendix. Close to coherent equilibrium ($\alpha \to \alpha_{c0}$), asymptotic behavior is $\Delta G^* \sim (\alpha - \alpha_{c0})^{-4}$, which is also consistent with the classical theory for martensitic nucleation.

The divergence of the nucleus size and vanishing of the nucleation energy barrier as the condition for lattice instability is approached are key features of the nonclassical nucleation in martensitic phase transformations captured by the extended model.

### B. *Homogeneous Martensitic Nucleation in the Fe-Co System*

One means of assessing the practical value of the foregoing model is to apply it to a real material system for which relevant parameters are available. Coherent homogeneous martensitic nucleation has been observed in defect-free Fe-Co particles precipitated from a Cu matrix.[15] On cooling, these small particles reach the very high levels of driving force which allow the homogeneous fcc → bcc transformation to occur, without being pre-empted by heterogeneous nucleation events which would occur at lower driving forces in larger particles with defects.

In the case of the fcc → bcc transformation, the geometry can be easily understood in terms of the Bain correspondence,[4] in which the product bcc state is achieved by a flattening of the initial fcc cubes in a direction parallel to a cube edge, which becomes the tetragonal axis of the product phase. In order to achieve the correct bcc geometry, this edge must be contracted by 29 pct relative to those which lie in the tetragonal basal plane. Allowing for a 4 pct volume increase, as indicated by Lin *et al.*,[15] we find that the transformation strain of this system corresponds to the values $\hat{\epsilon}_{11}^* = 0.14$ and $\zeta = -2.43$ in Eq. [24]. Additional data from this article indicate an elastic shear modulus of $\mu = 6.0 \times 10^{10}$ N/m$^2$ and a Poisson ratio of $\nu = 0.33$ for this system. The corresponding Lamé constant ($\lambda$) is then $1.16 \times 10^{11}$ N/m$^2$, and the application of Eq. [25] reveals that the habit plane lies at an angle of 48 deg to the tetragonal axis, close to the fcc (111) plane.

The nucleation energy barrier for the fcc → bcc transformation has the same form as Eq. [32] for a cubic-to-tetragonal transformation.[15] Therefore, the radii of the critical nucleus and the nucleation energy barrier are represented by Eqs. [33] through [35], respectively, and the normalized center strains of the critical nucleus are represented by Eq. [36]. The material parameters used in the experimental analysis of Lin *et al.* are summarized in Table I. Also in this table is an additional parameter, the critical driving force for lattice instability ($\Delta G_{vi}$), taken from the numerical work of Krasko and Olson[24] for pure Fe. The driving force for lattice instability is not expected to be sensitive to alloy composition.

Using the data from Table I and Eqs.[33] through [36], we find that

$$\epsilon_{ij}(0) = (0.45)^{(1-n)/2}(1 - \alpha)^{(n-1)/2} \quad [38]$$

$$a^* = 0.0310(\alpha - 0.55)^{-2}(1 - \alpha)^{(m-n)}\ \text{(nm)} \quad [39]$$

$$c^* = 0.0097(\alpha - 0.55)^{-1}(1 - \alpha)^{(m-n)}\ \text{(nm)} \quad [40]$$

$$\Delta G^* = 2 \times 10^{-23}(\alpha - 0.55)^{-4}(1 - \alpha)^{(3m-2n)}\ \text{(J)} \quad [41]$$

The radii $a^*$ and $c^*$ and the nucleation energy are plotted as functions of the driving force in Figures 9 and 10, respectively, for the case of $n = 3$ and $m = 2.5$. These values provide for the correct asymptotic behavior of the nucleus size and energy, as derived from the analysis of the cubic-to-tetragonal model of the previous section.

The nucleus shape, characterized by the ratio

$$\chi^* \equiv c^*/a^* = 0.3(\alpha - 0.55) \quad [42]$$

tends toward a very thin, platelike nucleus in the limit of coherent equilibrium ($\chi \to 0$ as $\alpha \to \alpha_{c0} = 0.55$) and is

**Table I. Material Data for the Fcc → Bcc Transformation in the Fe-Co System**

| $\Gamma$ | 0.01 (J/m$^2$) |
|---|---|
| $\Delta G_{s1}$ | 0.019 $\mu$ |
| $\Delta G_{s2}$ | 0.055 $\mu$ |
| $\Delta G_{vi}$ | −14.072 (kJ/mol) |
| $\mu$ | $6.0 \times 10^{10}$ (N/m$^2$) |
| $V_{\text{fcc}}$ | $6.82 \times 10^{-6}$ (m$^3$/mol) |

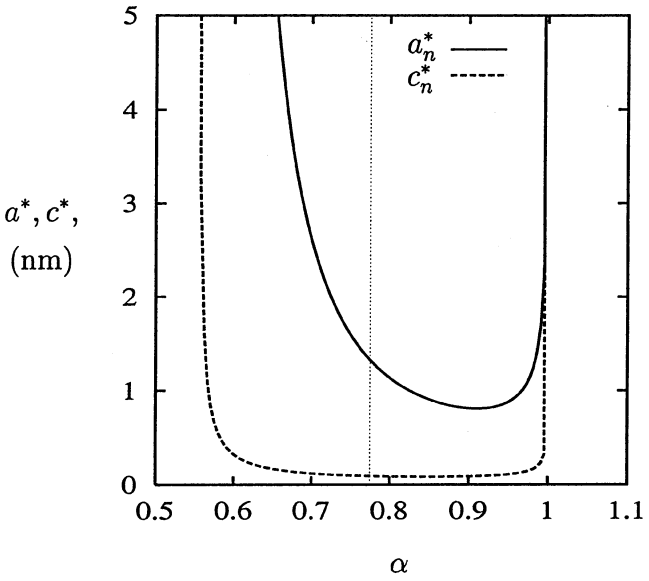


Fig. 9—Radii of the critical nucleus plotted as functions of the normalized driving force, $\alpha$, for homogeneous nucleation of the fcc → bcc transformation in the Fe-Co system.

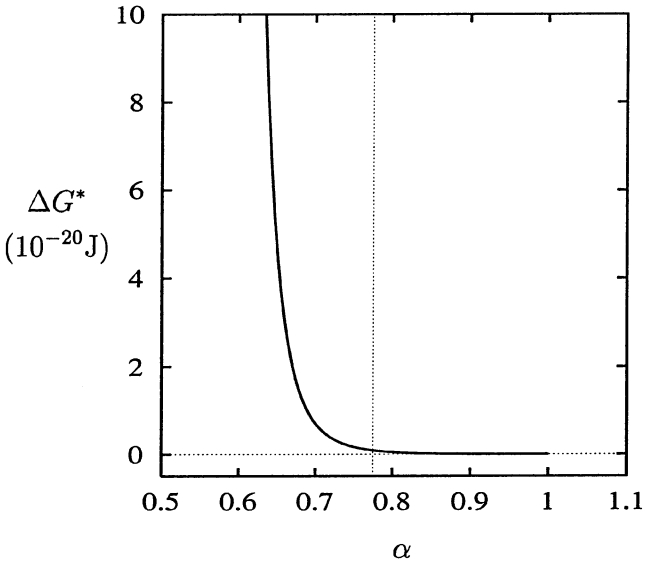


Fig. 10—Nucleation energy barrier plotted as a function of the normalized driving force, $\alpha$, for homogeneous nucleation of the fcc → bcc transformation in the Fe-Co system.

equal to 0.14 at the lattice instability point, $\alpha = 1$. Although the behavior between these two extremes is not monotonic, it is fair to say that the very thin, platelike nucleus is characteristic of the classical regime, whereas the nonclassical regime of higher driving forces gives rise to critical nuclei with a lower aspect ratio. The critical nucleus is, however, always an oblate spheroid.

In the Fe-Co system, using the data of Lin *et al.*[15] it is possible to make a quantitative assessment of the magnitude of nonclassical effects. The classical analysis that Lin *et al.* undertook to assess their data can be repeated with the new, nonclassical model, and a direct comparison can be made. In Figure 11, the data points from the paper of Lin *et al.* for combinations of driving force and temperature where

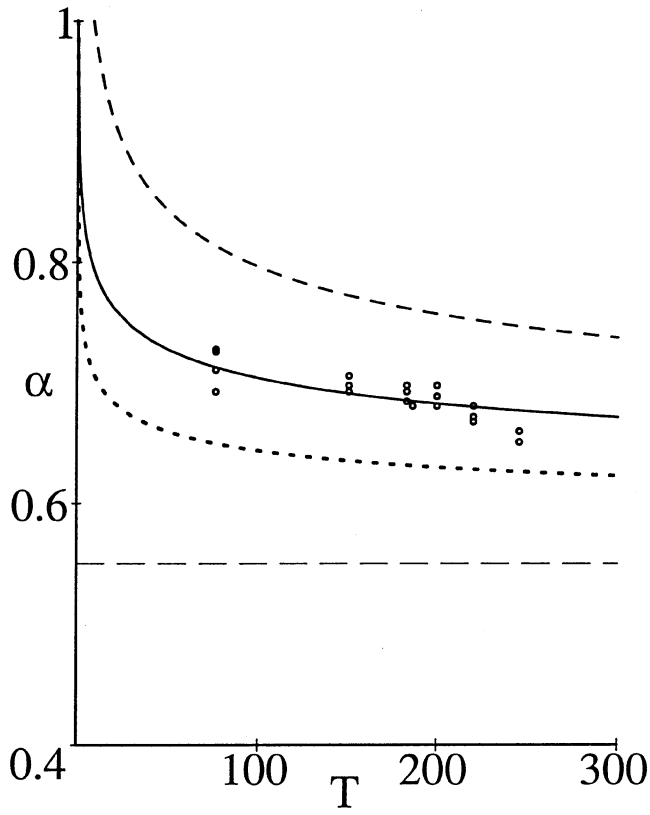


Fig. 11—Critical driving force for homogeneous, coherent nucleation in Fe-Co as a function of temperature. Circles are data from the article of Lin *et al.*[15] The lower dotted line is the prediction of the nonclassical nucleation model with the material parameters taken directly from Lin *et al.* The solid line is a fit of the nonclassical model to the data of Lin *et al.*, using the surface energy $\Gamma$ as a fitting parameter. Best fit is achieved when $\Gamma = 0.021$ J/m$^2$, roughly twice the value used in the classical model. The upper dashed curve is the classical nucleation model of Lin *et al.* using the fitted surface energy value. The lighter, horizontal line marks the equilibrium driving force $\alpha_{e0} = 0.55$. The difference between the solid curve and the upper dashed curve provides a measure of the effect of nonclassicality in this system.

homogeneous martensitic nucleation actually occurred, are plotted. Nucleation occurred in this system over a range of temperatures because of variations in composition of the precipitate particles. Estimating nucleation-rate prefactors, the critical driving force for nucleation was defined as the driving force, within a classical nucleation model, which satisfies the criterion that the barrier energy of the critical nucleus is

$$\Delta G^* = 40 k_B T \qquad [43]$$

where $k_B$ is the Boltzmann's constant.

Simple substitution of these classical model parameters into the new model, using the material constants of Table I, gives rise to critical driving forces indicated by the lower dotted curve of Figure 11. This lowers the predicted critical driving force for nonclassical nucleation relative to the classical model with the same parameters.

The central solid curve of Figure 11 results from a fit of the new model to the data of Lin *et al.*,[15] using the equilibrium surface energy as a fitting parameter. The surface energy is increased in order to compensate for the lowered bulk elastic energy of the nonclassical nucleus, and the result is an approximate doubling of the predicted surface energy, from

$\Gamma = 0.01$ to 0.021, when a minimal least-squares fit to the experimental data is achieved. This remains within the range of sensible values for coherent nucleation.

A repeat of the classical analysis of Lin *et al.*, with the new surface energy of $\Gamma = 0.021$ derived from the fit described previously, gives rise to the upper dashed curve of Figure 11. This classical curve diverges at zero temperature, in contrast to the nonclassical curves, which meet the $\alpha$-axis at $\alpha = 1$. The difference between this upper curve and the central, solid curve and data points is a measure of the reduction of the critical driving force required for homogeneous, coherent martensitic nucleation due to nonclassical effects. Over the range of experimental observations ($0.65 < \alpha < 0.75$), this constitutes a significant reduction of approximately 20 pct.

Based on Eq. [38], the corresponding level of $\eta^*$ is 0.55 to 0.75 in the approximate model. The extended model overestimates the departure of the nucleus strain amplitude from the classical case. One must, of course, be cautious in generalizing this behavior to the cubic-to-tetragonal model, but, for a critical $\alpha$ value in the vicinity of 0.7, Figure 6 suggests that the $\eta^*$ value achieved by the nonclassical nucleus may be as low as 0.5 in this model, as compared to that of 0.9 for the corresponding Landau–Ginzburg model. These are both nonclassical critical nuclei, and the new model does an excellent job of tracking the other relevant parameters (critical nucleus size and energy), indicating a 20 pct reduction in the critical driving force for nucleation.

## V. CONCLUSIONS

We have developed a technique which extends the range of validity of classical nucleation theory into the nonclassical regime by introducing driving-force dependencies to the interfacial free energy, the misfit strain energy, and the nucleus chemical free energy. These driving-force dependencies are determined by matching the asymptotic behavior of the extended model with respect to nucleus size and nucleation energy barrier to the corresponding solutions of the Landau–Ginzburg model in the highly nonclassical limit of lattice instability. No additional material parameters other than those used in the classical and Landau–Ginzburg models are required, and the form of most of the analytical solutions can be easily obtained from the well-understood behavior of the classical theory.

This extended model compares favorably with nonlinear nonlocal models of the Landau–Ginzburg type in the nonclassical regime, for the particular case of nucleation in a dilatational phase transformation. Both the extended model and the Landau–Ginzburg model capture the nonclassical nucleation phenomena, including divergence of the nucleus size and vanishing of the nucleation energy barrier as the condition for lattice instability is approached, and match well with each other. However, the new extended model has the substantial advantage of giving closed-form analytical solutions, which are highly desirable from a computational perspective.

In the case of homogeneous nucleation of a fully coherent cubic-to-tetragonal phase transformation, the nonclassical nucleation phenomena predicted by this model are consistent with the corresponding asymptotic solutions of the associated Landau–Ginzburg model in the vicinity of lattice instability. The cubic-to-tetragonal transformation offers an additional feature, in that the transformation is necessarily accompanied by a (nucleus) shape-independent misfit strain energy per particle volume. This shape-independent strain energy is 3D in character and causes a higher driving force for nucleation of the cubic-to-tetragonal phase transformation. Computationally tractable access to the nonclassical regime in high-dimensional systems is crucial to modeling this effect.

We have also applied this new extended model to the nonclassical homogeneous nucleation behavior of an experimental system, specifically the fcc → bcc transformation in the Fe–Co system. This system nucleates in the nonclassical regime, and our computations indicate that the nucleation critical driving force predicted from the extended, nonclassical model is about 20 pct lower than that predicted from simple classical considerations, providing a quantitative demonstration of the importance of nonclassicality in an experimental system.

## ACKNOWLEDGMENTS

The authors are grateful for the support of the National Science Foundation through Grant Nos. MSS-9313233 and DMR-9500122 to Northwestern University.

## APPENDIX
## Asymptotic solutions of the Landau–Ginzburg model near the lattice instability

The nonclassical nucleation behavior predicted by the Landau–Ginzburg approach for phase transformations from one to three dimensions is derived. The asymptotic behavior in the nucleation energy barrier in the vicinity of lattice instability depends on the types of the Landau potentials. In this appendix, we focus on two frequently used Landau potentials, *i.e.*, the 2-3-4 potential and the 2-4-6 potential.

### A. *The 2-3-4 Landau–Ginzburg Potential*

The nucleation energy barrier based on a 2-3-4 type Landau–Ginzburg potential is written as

$$\Delta G = \int_{\Omega} \left( A\eta_1^2 - B\eta_1^3 + C\eta_1^4 + \sum_{\gamma} D_\gamma \eta_\gamma^2 + \kappa(\nabla_x \eta_1)^2 \right) dV_x \quad [A1]$$

where $\Omega$ represents an infinite domain, $\eta_1$ is the major-order parameter associated with the transformation (*e.g.*, the normalized volumetric strain for a dilatational transformation), $\eta_\gamma$ represents the required minor-order parameters associated with the transformations, $\nabla_x \eta_1$ is the gradient of the major-order parameter with respect to the coordinate system $x_i$, and $A$, $B$, $C$, $D_\gamma$, and $\kappa$ are material constants. Note that close to lattice instability ($\alpha \rightarrow \alpha_i$), the order parameters $\eta_1 \rightarrow 0$ and $\eta_\gamma \rightarrow 0$, since the energy-density barrier is vanishing.* Introducing a set of dimensionless order parameters,

*In general, $\alpha = \alpha_i = 1$ at lattice instability.[9]

$$Y_1 = \frac{B}{A}\,\eta_1 \qquad [A2a]$$

$$Y_\gamma = \frac{BD_\gamma^{1/2}}{A^{3/2}}\,\eta_\gamma \qquad [A2b]$$

and a dimensionless coordinate system,

$$\xi_i = \left(\frac{A}{\kappa}\right)^{1/2} x_i \qquad [A3]$$

the nucleation energy barrier in Eq. [A1], neglecting the higher-order term $\eta_1^4$, can be rewritten as

$$\Delta G_{(\alpha\rightarrow\alpha_i)} = \frac{A^{(3-s/2)}\kappa^{s/2}}{B^2}\int_\Omega \left(Y_1^2 - Y_1^3 + \sum_\gamma Y_\gamma^2 + (\nabla_\xi Y_1)^2\right) dV_\xi \qquad [A4]$$

where $dV_\xi = (A/\kappa)^{s/2}\,dV_x$ and $s$ represents the spatial dimensions associated with the considered transformations (*i.e.*, $s = 1, 2,$ or 3 for one, two, or three dimensions, respectively). The integral in Eq. [A4] is not only dimensionless but also independent of the driving-force dependencies of the material constants, since the Euler–Lagrange equations associated with the stationarity of the nucleation energy barrier in Eq. [A4] are dimensionless. Note that, in the 2-3-4 potential, $A \rightarrow 0$ but $B$ remains finite as $\alpha \rightarrow \alpha_i$. Therefore, it can be shown that, for $A \sim (\alpha_i - \alpha)$ and a constant $\kappa$,

$$\Delta G_{(\alpha\rightarrow\alpha_i)} \sim (\alpha_i - \alpha)^{(3-s/2)} \qquad [A5]$$

*i.e.*, $\Delta G^{1\text{-D}}_{(\alpha\rightarrow\alpha_i)} \sim (\alpha_i - \alpha)^{5/2}$, $\Delta G^{2\text{-D}}_{(\alpha\rightarrow\alpha_i)} \sim (\alpha_i - \alpha)^2$ and $\Delta G^{3\text{-D}}_{(\alpha\rightarrow\alpha_i)} \sim (\alpha_i - \alpha)^{3/2}$ for one-dimensional (1 D), 2-D, and 3-D phase transformations, respectively. Defining the radii of the critical nucleus along the $x_j$ directions to be $R_j^* = x_j^* = (\kappa/A)^{1/2}\xi_j^*$, it can be shown that, close to lattice instability, the driving-force dependence of the radii of the critical nucleus is

$$R^*_{j(\ \alpha\rightarrow\alpha_i)} \sim (\alpha_i - \alpha)^{-1/2} \qquad [A6]$$

which is valid for transformations from one to three dimensions. It can be seen from Eqs. [A5] and [A6] that, as $\alpha \rightarrow \alpha_i$, the nucleation energy barrier tends to zero (with different rates of convergence), but the radii of the critical nucleus tend to infinity (with the same rate of divergence), which are key features associated with the nonclassical nucleation.

### B. *The 2-4-6 Landau–Ginzburg Potential*

The nucleation energy barrier based on a 2-4-6 type Landau–Ginzburg potential is written as

$$\Delta G = \int_\Omega \left(A\eta_1^2 - \hat{B}\eta_1^4 + \hat{C}\eta_1^6 + \sum_\gamma D_\gamma \eta_\gamma^2 + \kappa(\nabla_x \eta_1)^2\right) dV_x \qquad [A7]$$

where $\hat{B}$ and $\hat{C}$ are material constants. Introducing another set of dimensionless order parameters,

$$Z_1 = \left(\frac{\hat{B}}{A}\right)^{1/2} \eta_1 \qquad [A8a]$$

$$Z_\gamma = \frac{\hat{B}D_\gamma^{1/2}}{A^{3/2}}\,\eta_\gamma \qquad [A8b]$$

and using Eq. [A3], the nucleation energy barrier in Eq. [A7], neglecting the higher-order term $\eta_1^6$, can be rewritten as

$$\Delta G_{(\alpha\rightarrow\alpha_i)} = \frac{A^{(2-s/2)}\kappa^{s/2}}{\hat{B}^2}\int_\Omega \left(Z_1^2 - Z_1^4 + \sum_\gamma Z_\gamma^2 + (\nabla_\xi Z_1)^2\right) dV_\xi \qquad [A9]$$

Therefore, it can be shown that, for $A \sim (\alpha_i - \alpha)$ and a constant $\kappa$,

$$\Delta G_{(\alpha\rightarrow\alpha_i)} \sim (\alpha_i - \alpha)^{(2-s/2)} \qquad [A10]$$

*i.e.*, $\Delta G^{1\text{D}}_{(\alpha\rightarrow\alpha_i)} \sim (\alpha_i - \alpha)^{3/2}$, $\Delta G^{2\text{D}}_{(\alpha\rightarrow\alpha_i)} \sim (\alpha_i - \alpha)^1$, and $\Delta G^{3\text{D}}_{(\alpha\rightarrow\alpha_i)} \sim (\alpha_i - \alpha)^{1/2}$ for 1-D, 2-D, and 3-D phase transformations, respectively. It also can be shown that, close to lattice instability, the asymptotic behavior in the radii for the 2-4-6 model is the same as that of the 2-3-4 model shown in Eq. [A6].

## REFERENCES


1. J.C. Fisher, J.H. Hollomon, and D. Turnbull: *Trans. AIME*, 1949, vol. 185, pp. 691-700.
2. L. Kaufman and M. Cohen: in *Progress in Metal Physics*, B. Chalmers and R. King, eds., Pergamon Press, New York, NY, 1958, vol. 7, pp. 165-246.
3. J.W. Christian: *The Theory of Transformations in Metals and Alloys*, 2nd ed., Pergamon, Oxford, United Kingdom, 1975.
4. D.A. Porter and K.E. Easterling: *Phase Transformations in Metals and Alloys*, 2nd ed., Chapman and Hall, London, 1992.
5. G.B. Olson and A.L. Roitburd: in *Martensite*, G.B. Olson and W.S. Owen, eds., ASM INTERNATIONAL, Materials Park, OH, 1992.
6. A.L. Roitburd: in *Solid State Physics*, H. Ehrenreich, F. Seitz, and D. Turnbull, eds., Academic Press, New York, NY, 1978, vol. 33, pp. 317-90.
7. G.B. Olson and M. Cohen: *J. Phys.*, 1982, vol. 43, pp. C4-C5.
8. D.M. Haezebrouck: Ph.D. Thesis, Massachusetts Institute of Technology, Cambridge, MA, 1987.
9. B. Moran, Y.A. Chu, and G.B. Olson: *Int. J. Solid Structure*, 1996, vol. 33 (13), pp. 1903-19.
10. Y.A. Chu and B. Moran: *Modelling Simul. Mater. Sci. Eng.*, 1995, vol. 3, pp. 455-71.
11. T. Belytschko, Y.Y. Lu, and L. Gu: *Int. J. Num. Methods Eng.*, 1994, vol. 37, pp. 229-56.
12. Y.Y. Lu, T. Belytschko, and L. Gu: *Comput. Methods Appl. Mech. Eng.*, 1994, vol. 113, pp. 397-414.
13. G.R. Barsch and J.A. Krumhansl: *Phys. Rev. Lett.*, 1984, vol. 53(11), pp. 1069-72.
14. G.R. Barsch and J.A. Krumhansl: *Metall. Trans. A*, 1988, vol. 19A, pp. 761-75.
15. M. Lin, G.B. Olson, and M. Cohen: *Acta Metall. Mater.*, 1993, vol. 41(1), pp. 253-63.
16. J.D. Eshelby: *Proc. R. Soc.*, 1957, vol. A241, pp. 376-96.
17. J.D. Eshelby: *Proc. R. Soc.*, 1959, vol. A252, pp. 561-69.
18. T. Mura: *Micromechanics of Defects in Solids*, 2nd ed., Academic Publishers, Hingham, MA, Kluwer, 1987.
19. J.W. Cahn and J.E. Hilliard: *J. Chem. Phys.*, 1958, vol. 28, pp. 258-67.
20. P. Hong: Ph.D. Thesis, Northwestern University, Evanston, IL, 1994.
21. P. Hong and G.B. Olson: *Solid State Commun.*, 1993, vol. 85(8), pp. 681-83.
22. S.H. Wen, E. Kostlan, M. Hong, A.G. Khachaturyan, and J.W. Morris, Jr.: *Acta Metall.*, 1981, vol. 29, pp. 1247-54.
23. Y.A. Chu: Ph.D. Thesis, Northwestern University, Evanston, IL, 1996.
24. G.L. Krasko and G.B. Olson: *Phys. Rev. B*, 1989, vol. 40(17), pp. 11536-11545.
25. A.G. Khachaturyan: *Theory of Structural Phase Transformations in Solids,* John Wiley and Sons Inc., New York, 1983.